AGRICULTURE AND NATURAL RESOURCES

Journal homepage: http://anres.kasetsart.org

Research article

Comparison of drone with remote-controlled sprayer arm and variable rate sprayer for monitoring coconut rhinoceros beetle infestations

Grianggai Samseemoung[a,*], Junlaphong Bhucksasri[a], Sunan Parnsakhorn[a], Roongruang Kalsirisilp[a], Malarin Samseemung[b], Hemantha PW Jayasuriya[c]

[a] *Department of Agricultural Engineering, Faculty of Engineering, Rajamangala University of Technology Thanyaburi, Pathum Thani 12110, Thailand*

[b] *Sub ICU-CVT Department, Maharaj Nakorn Chiang Mai Hospital, Chiang Mai 50200, Thailand*

[c] *Department of Soils, Water & Agricultural Engineering, College of Agricultural & Marine Sciences, Sultan Qaboos University, Al-khod Sultanate of Oman 123, Oman*

Article Info

Article history:
Received 12 October 2022
Revised 20 February 2023
Accepted 21 February 2023
Available online 30 April 2023

Keywords:
Coconut tree,
Drone with sprayer arm,
Image processing,
Three-way analysis of variance,
Variable rate sprayer

Abstract

Importance of the work: Drones are now widely available, inexpensive, and adaptable. Additional equipment can be used for precision or smart agriculture, especially in the spraying of coconut rhinoceros beetle infestations, and to reduce the risk of direct chemicals.

Objectives: To design, fabricate and compare the performance of a remote-controlled sprayer arm with a drone-mounted, variable-rate (VRT) sprayer for rhinoceros beetle monitoring. Image data segmentation was compared by calibrating the altitude of the camera and nozzle.

Materials & Methods: The drone used had a payload capacity of 5 kg, weighed roughly 7.85 kg and was flown using a radio transmitter with a range of 1–2 km. The equipment was attached to the sprayer arm, which had a camera and a spray nozzle with a variable spray rate control system. The remote control could be operated from the ground and benchmark comparisons were made with a ground-based variable rate sprayer to determine a working speed, working capacity, spraying rate, electricity consumption and fuel consumption.

Results: With a working speed of 1.25 km/hr and a spraying rate of 0.333 L/hr, the drone had a working capacity of 0.352 ha/hr and consumed 0.741 kWhr of electricity. There was a significant correlation between either the normalized difference vegetation index captured by the drone ($NDVI_{Drone}$) or the green normalized difference vegetation index ($GNDVI_{Drone}$) and the chlorophyll detected using a chlorophyll meter in both healthy and infected mature coconut trees (Pearson's correlation coefficient, (r) in the range 0.7885−0.8126). The VRT sprayer had a fuel consumption of 0.58 L/hr, a working capacity of 0.056 ha/hr, and a spraying rate of 162.72 L/hr at a forward speed of 1.5 km/hr for healthy and infected mature coconuts. High correlations were observed between either the normalized difference vegetation index for the sprayer ($NDVI_{VTR\ Sprayer}$) or the green normalized difference vegetation index for the sprayer ($GNDVI_{VTR\ Sprayer}$) and the chlorophyll content measured using a chlorophyll meter in both healthy and infected trees (r range = 0.8288−0.9595).

Main finding: The benefit of using a drone with a sprayer arm was that numerous coconut trees could be sprayed, with less transportation required of chemicals. The drawback of the VRT sprayer was that spraying could only be carried out extremely slowly. However, it had a large chemical carrying capacity.

* Corresponding author.
E-mail address: grianggai.s@en.rmutt.ac.th (G. Samseemoung)

https://doi.org/10.34044/j.anres.2023.57.2.05

Introduction

A variable rate (VRT) chemical sprayer was created and evaluated to address: 1) the difficulties associated with conventional chemical spraying; and 2) the goals of boosting plantation yield, lowering production costs and minimizing the environmental and health risks of excessive chemical usage. Sprayers use image processing techniques (Jarimopas and Jaisin, 2008; Sirisomboon et al., 2009; Samseemoung et al., 2011; 2012; 2016; 2017a, b; Sirikun et al., 2021; Indarto et al., 2022;) to control disease and pest infestations in coconut farms (Office of Agricultural Economics, 2020) and offer efficient pest management. However, the difficulty of spraying chemicals by hand into the high crown of a coconut palm has led to the rapid development of and intense market rivalry between drones so that drone performance has increased and there is a gradual declining trend in prices (Samseemoung et al., 2023). In addition, drones are being utilized increasingly for agricultural tasks, such as spraying insecticides over rice fields and surveying planting regions. In response to these issues, the current study aimed to design, fabricate and compare the performance of a remote-controlled sprayer arm with a drone-mounted and variable-rate (VRT) sprayer for monitoring coconut rhinoceros beetle infestations and assisting coconut growers.

This study compared the strengths of using a remote-controlled sprayer arm with a drone-mounted, VRT sprayer to monitor coconut rhinoceros beetle infestations. The GPS receiver location of the coconut was tested in the plots impacted by the borer outbreak, along with system performance. Finally, the use of suitable software was investigated to help coconut farmers to develop a GIS agricultural application map that could serve as a database for them to utilize in the future.

Materials and Methods

Hardware and system setup for drone with remote-controlled sprayer arm and variable rate sprayer and preparing the field experiment setup

To prevent excessive jerks during picture capture, the drone speed was kept low when using a variable rate sprayer in the low-dynamic mode of image data collection. A commercial drone was chosen for the high-dynamic mode of image data capture (model #GCS-9 Lipo Battery 6S1P 14,000 mAh 22.2 V; KASET GEN Y Co., Ltd.; Thailand). It had a payload capacity of 5 kg, weighed roughly 7.85 kg and was flown by an experienced pilot using a radio transmitter with a range of 1–2 km. The essential elements of both low-altitude remote sensing (LARS) platforms used in the study are shown in Fig. 1.

This research collected data from coconut plantation test plots (at 14.42°N, 100.48 °E in Bueng Bon, Nong Suea district, Pathum Thani province, Thailand) where a large number of coconut borer infestations had occurred. The coconut planting plots were planted at a distance between trees of 9 m and a distance between rows of 7.8 m. All tests were performed in an experimental plot of 40 m × 40 m. Fertilizers were applied at the rates of 59–91 kg/ha for nitrogen, 27–40 kg/ha for phosphorus and 85–131 kg/ha for potassium, respectively. The soil physical characteristics are listed in Table 1 for the location and in Table 2 for the comparison of the two parameters. The tests were conducted only when the wind speed was low, which was determined from the movement of the top of the coconut trees. The test route was moved along the length of the coconut plantation.

Table 1 Physical characteristics of soil and fertilizer rates used in coconut plantations

Coconut age (yr)	Rate of N:P:K fertilizer at 13:13:21 or 12:12:17 (kg/m^2)	Magnesium sulfate (kg/m^2)	Dolomite (kg/m^2)
1	1	0.2	-
2	2	0.3	2
3	3	0.4	3
4 or more	4	0.5	4
Soil depth (cm)	0–20		
pH	6–7		
Soil texture	Clay		
Sand (%)	15		
Silt (%)	30		
Clay (%)	55		
Organic matter (%)	1.54		
Particle density (g/cm^3)	2.42		
Bulk density (g/cm^3)	1.37		
Moisture content (%, dry basis)	23		

Table 2 Comparison of various parameters between local drone and variable rate sprayer

Parameter	Variable rate sprayer	Local drone
Manpower	2	2
Pressure (MPa)	0.15	0.4
Pollution	Yes	No
Energy need	Yes	Yes
Speed (km/hr)	1.5	1.26
Altitude range (m)	5–9	5-2,000
Actual working performance (ha/hr)	0.056	0.352
Fuel consumption rate	0.58 L/hr	15 min/battery
Spraying rate (L/hr)	162.72	0.333
Price (USD)	896.08	2,091.19
Usable by elderly person	No	Yes

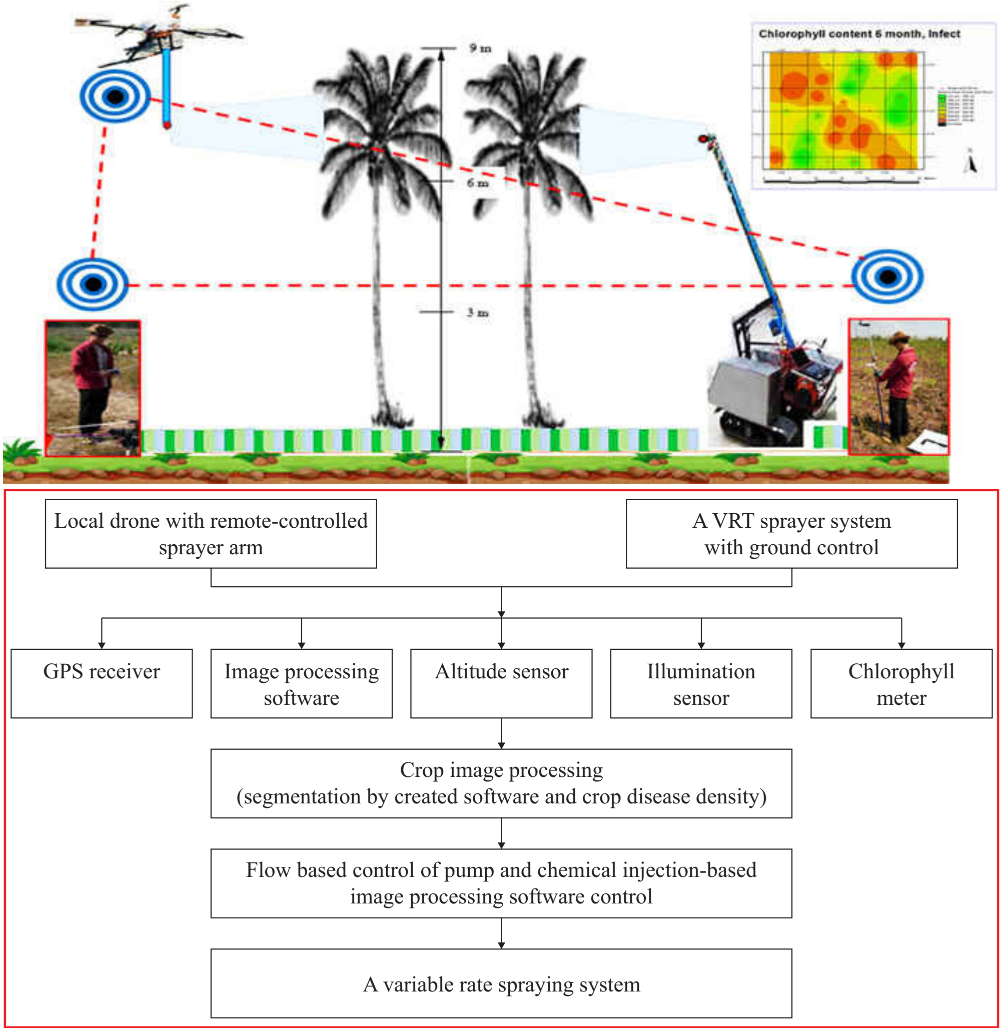

Fig. 1 Design and fabrication of hardware and system configuration in low-altitude remote sensing (LARS) systems

Method for acquiring image data and a different signal receiver sensor of a drone with remote controlled sprayer arm and a variable rate sprayer

The system platform consisted of a WebCAM camera (Vimicro USB2.0 UVC PC Camera; Swift-tech Electronics Co. Ltd.; China), an illumination sensor (two channels with central bands at 660 nm and 730 nm; Skye Instruments; UK), an altitude sensor (Seagull Wireless Dashboard Flight System FCC 900 MHz version; UK), a central processing unit (CPU) for the computer and control software (Research Systems, Inc.; USA). The specially created software offered normalized difference vegetation index (NDVI) analysis, geo-referencing and image orientation correction. The intensity of the prevailing sun was measured using an SKR 1800 lighting sensor (UK). A data logger had an illumination sensor attached to it (SpectroSense-2; Skye Instruments; UK). The LARS platform's altitude was measured and controlled using a wireless altitude sensor to capture photographs from a fixed altitude. Latitude and longitude coordinates were recorded using a GPS receiver (Garmin Legend H Handheld GPS Navigator 24 MB of internal memory, with a high-sensitivity WAAS-enabled GPS receiver; Garmin Ltd.; USA). ArcGIS® software using a GIS application to map infected crop areas was produced that contained geographic data on the fields (Astanakulov et al., 2021). During the experiment, the average chlorophyll content (expressed as SPAD values) of coconut leaves was measured using a leaf chlorophyll meter (Minolta SPAD 502; Konica Minolta Sensing Inc.; Japan) for calibration and ground truthing. The equation to describe the units for the Minolta SPAD-502 leaf chlorophyll meter (Markwell et al., 1995) is provided in Equation 1:

$$Chl\ \mu mol\ m^{-2} = 10^{M\,0.265} \qquad (1)$$

where, *M* is the leaf chlorophyll meter reading (a digital number) and *Chl* is the chlorophyll content in micro moles per square meter.

GNDVI values were computed to determine the appropriateness of this reflectance measure for coconut plantations during various tree growth phases. The GNDVI, which measures the level of greenness and represents the chlorophyll content (as measured by radiance at the leaf surface), is an important indicator to differentiate healthy coconut palms from infected ones. According to Gitelson et al. (1996), the GNDVI is calculated using Equation 2:

$$GNDVI = \frac{\rho NIR - \rho G}{\rho NIR + \rho G} \quad (2)$$

where ρNIR is the reflectance value for the near infrared band and ρG is the reflectance value for the green band.

Monitoring coconut rhinoceros beetle infected acquisition and processing image data from both systems

Data on the infestation of coconut rhinoceros beetles was gathered from the upper crowns of the coconut trees. Subsequently, the chemical sprayer with remote monitoring devices was designed using the information gathered. *Bacillus thuringiensis* subsp. *aizawai*, a chosen biocontrol agent, was evaluated to determine the most suitable dose to produce the maximum efficiency while being operator-safe at rates of 80-100 cm^3 in 20 L of water. In addition, current pest management methods were investigated to clearly grasp how chemicals are used by farmers.

A Thai spraying drone (model #GCS-9 Lipo Battery 6S1P 14,000 mAh 22.2 V; Kaset Gen Y Co. Ltd.; Thailand) was used as the base on which the sprayer arm equipment was installed. Some of the main features were a diaphragm pump mechanism, a maximum flowrate of 210 L/hr, manual operation with remote control, a total weight of 7.85 kg and a spraying time of approximately 15 min per battery. The unit had eight propellers and could carry up to 5 L of liquid at a time and rise to an operational height of 30 m, The IP Camera (Smart IP Camera VSTARCAM C90S-A0131296 Lens: HLC-GC2053-V40-V2.0 module 2.4 GHz/ IEEE 802.11 b/g/n; Advice Co. Ltd.; Thailand) was used to record the spray photos and to keep track of the coconut beetle penetration targets. The spray nozzle was made of brass (Quick Jet Full Cone Spray Jet Nozzle Agriculture Nozzle; Huajue Sprayer Equipment Store; China). The spray nozzle operated at 2 bar pressure and a 108 L/hr flow rate. A strong, lightweight, aluminum frame was used in the design and fabrication of the drone and a remote-controlled spraying arm was installed. Assembling involved all of the following parts: pulleys (SP Series Pulley; Carl Stahl Sava Industries, Inc.; USA), steel wire rope sling (TOHO; China), motor (Gear-Box Motor, 12 VDC, 30 RPM; Warf electronics shopping; Thailand), reagent pipe (polyethylene tube, outside diameter of 4 mm), internal dowel sling fixing bolts (Bolt and Nut M-4; Standard 45; Thailand), sprayer arm, smart IP camera and spray nozzle, as shown in Fig. 2. The sprayer arm was mounted next to the drone and made of aluminum. The sprayer arm hangs loosely during take-off and landing in accordance with the operational theory so that it could be folded horizontally. When hovering and spraying, the sprayer arm is tightly secured to the sling, which improves spraying accuracy and makes it easier to manage.

The VRT sprayer was constructed by taking into account pertinent observations of trees, spraying procedures and the field of view. The mobility of the sprayer crane was made possible by using Caterpillar® tracks. The crane could extend to a height of 10 m. Two operators manually controlled the nozzle. The crane system, motors, power system, chemical tank and pump, crane system, nozzle with remote monitoring system, controlling system and crane control system were made up the sprayer's seven main parts. Carbon steel tubes, each 30.48 mm × 30.48 mm × 3,000 mm used to construct the crane system and were fixed with 40.64 mm × 40.64 mm × 3000 mm, 50.8 mm × 50.8 mm × 3000 mm and 55.88 mm × 55.88 mm × 3,000 mm carbon steel tubes to give it a maximum length of 10 m. When the tubes were brought together inward or outward, strings were fastened to each one, creating a telescopic crane boom. A wireless WebCAM was added at the nozzle to improve spraying accuracy and nozzle direction control. Crane elevation, chemical spraying and camera angle (field of view) adjustment were taken into consideration when designing the movement controller and crane, which is crucial for the operation of the sprayer and crane. An operator directed the sprayer toward the desired coconut tree to begin the procedure. When the crane boom reached the top of the coconut tree and the infestation target was established, the crane and motors were controlled. The chemical was poured into the infested region at a particular rate as the nozzle was aimed at the target using a remote monitoring system.

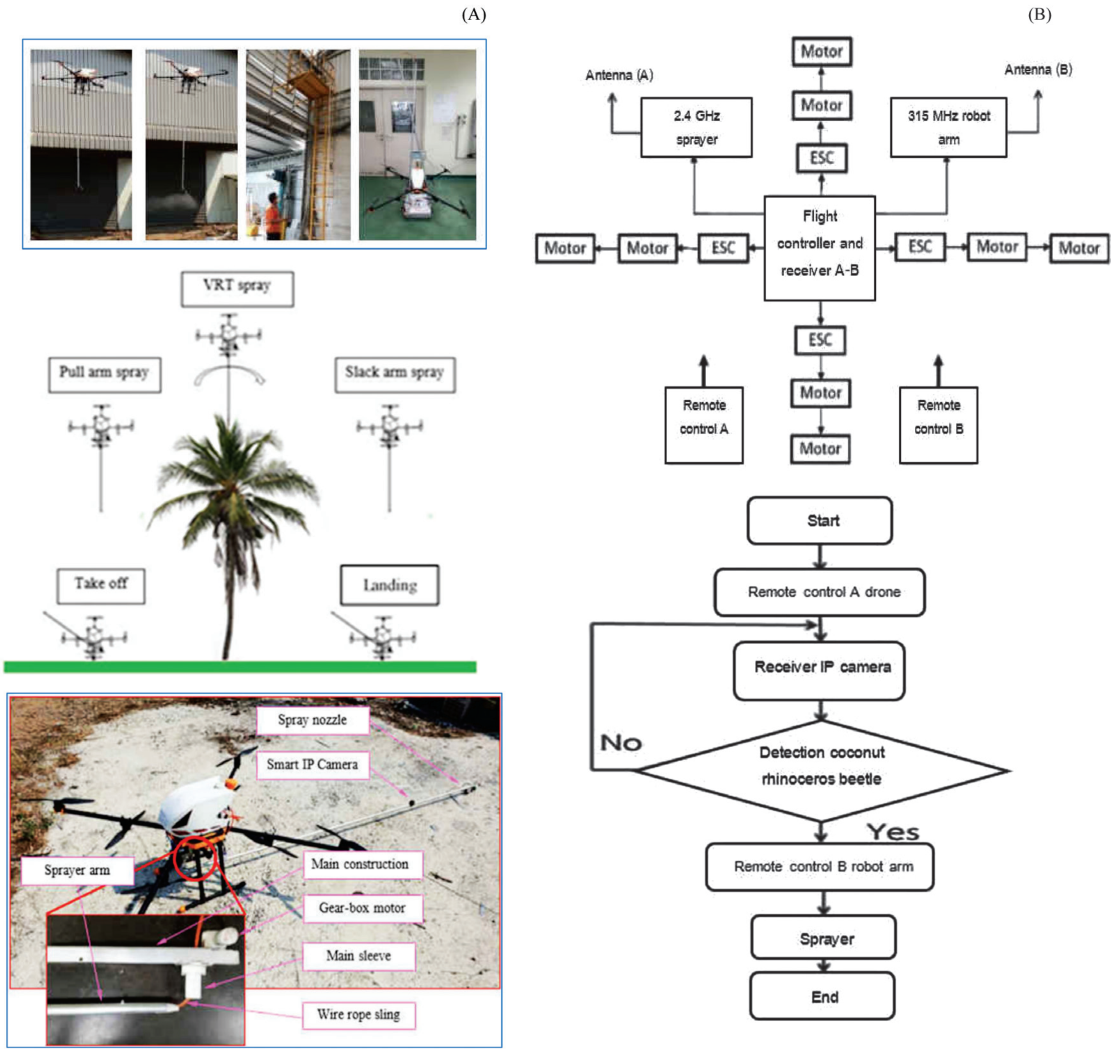

Fig. 2 Design and fabrication of hardware and system configuration for local drone, where VRT = variable rate

An algorithm was created to distinguish the object of interest from its background when processing images. The created software loads the WebCAM photos (in red-green-blue) and gives the user the option of selecting particular image profiles. The four zones of the chosen image are used by the developed software to estimate the infected density. Yellow and brown coconut shoots were discovered for analysis of the photos to determine the density percentage per area. The outcomes are shown on the program's screen. Then, the computer translates the colored images into grayscale images and calculates the solenoid valve's volume flow rate for nozzle injection. Finally, as illustrated in Fig. 3, the finalized photos are recorded on a hard drive (as a gray image and a bimodal image).

Image calibration of drone with remote controlled sprayer arm and variable rate sprayer

A conventional reference frame of 50 cm × 50 cm was used to evaluate the accuracy of a target covered by the spray for an appropriate spraying footprint (based on the diameter in centimeters) and nozzle altitude levels (measured in meters). Yellow cards with dimensions of 2.54 cm × 2.54 cm were used as samples to depict the diseases and pest infestation region in the reference frame. Three sample color groups were used in the trials: 25% (13 pieces), 50% (26 pieces) or 100% (52 pieces) held at 0.5 m, 0.7 m, 1 m or 2 m from the nozzle. Variations in illumination levels according to the time of day were also included in this calibration.

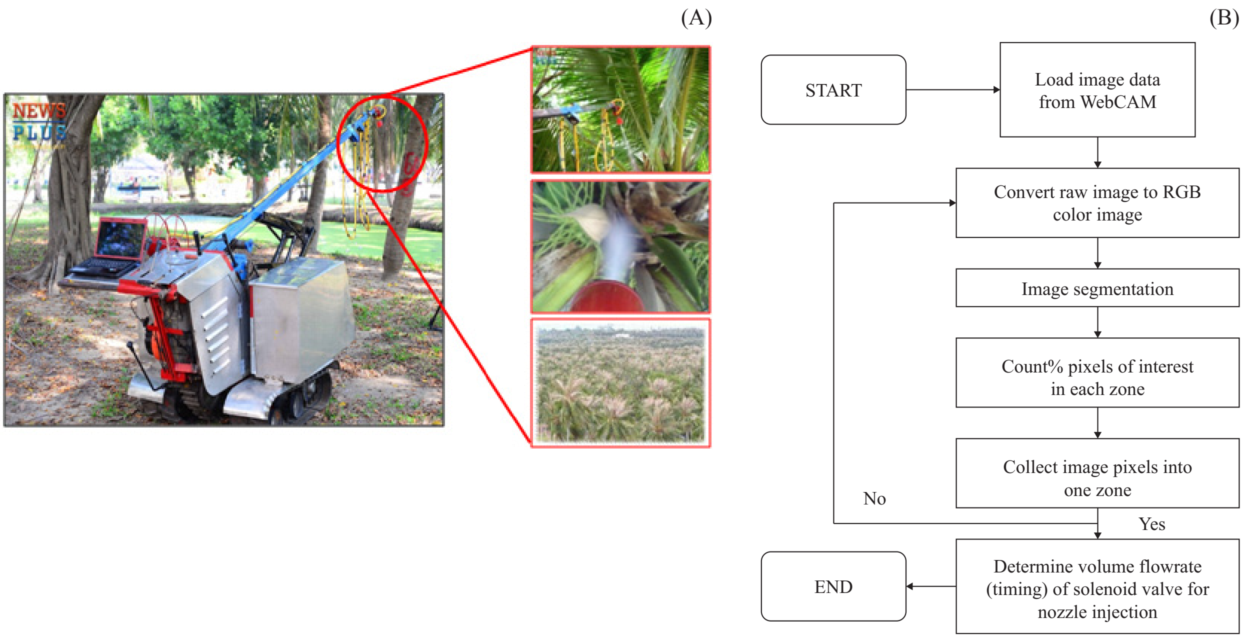

Fig. 3 Design and fabrication of a hardware and a variable rate (VRT) sprayer

Ground truthing measurements

The SPAD-502 chlorophyll meter and the GPS receiver were used for ground truthing. At a height of 9 m, measurements were made with both the crane-mounted and drone-mounted LARSs. A 40 m × 40 m area with a 7.8 m row spacing was chosen for GPS receiver measurements of the infected location in the coconut plantation. The operator was positioned between crop rows to measure the reflectance.

Field research and performance assessment

The capacity of the designed sprayer machine was assessed in the coconut plantation. The assessment took into account the capacity to operate at altitudes of up to 9 m, the actual working capacity of the sprayer (measured in hectares per hour), the fuel consumption of the sprayer (measured in liters per hour) and the electricity consumption of the sprayer (measured in kilowatts per hour).

Statistical analysis

A three-way analysis of variance was used, followed by a post-hoc test (Duncan's multiple range test), to determine the effects of three factors (the altitude of spraying, the density of the yellow color and the altitude levels of the nozzle) and the interactions of these three variables on the spraying footprint of a local drone with a sprayer arm. In addition, data collected using a VRT sprayer were analyzed using the same procedure. The three-way analysis of variance was carried out to determine the altitude of spraying, the density of yellow color and the altitude levels of nozzle and the interactions of these three variables for evaluation of the characteristics of the spraying footprint (diameter measured in centimeters). Pearson's correlation coefficients (r) between the chlorophyll content and either the NDVI or GNDVI were calculated for both datasets (from the drone and the VRT sprayer). All analyses were performed using Duncan's multiple range test and the tests were considered significant at $p < 0.05$.

Results and Discussion

System performance and calibration for image acquisition and processing

Local drone with sprayer arm

The chemical pump was tested at 0.4 MPa, with the resulting spraying flow rate of 0.333 L/hr. For the yellow sample, the spraying footprint was assessed with densities of 25% (13 pieces), 50% (26 pieces) or 100% (52 pieces) at nozzle heights of 1 m, 2 m, 3 m or 4 m. The diameter of the sprayed area was used to calculate the spraying footprint (Table 3).

Table 3 Spraying footprint diameter (in centimeters) of local drone with sprayer arm at different spraying and nozzle altitudes and yellow color sheet density percentages

Spraying altitude (m)	Density of yellow color (%)	Nozzle altitude (m)			
		1	2	3	4
5	25	42.00^{a}	55.00^{c}	69.33^{g}	110.00^{o}
	50	43.00^{ab}	56.67^{d}	69.67^{gh}	92.89^{l}
	100	43.67^{b}	56.67^{d}	70.33^{ghij}	113.31^{p}
7	25	42.00^{a}	58.33^{e}	71.00^{ijk}	94.67^{m}
	50	43.00^{ab}	57.67^{de}	70.00^{ghi}	93.34^{l}
	100	43.67^{b}	58.00^{e}	71.33^{jk}	116.10^{q}
9	25	42.00^{a}	59.67^{f}	71.00^{ijk}	95.10^{m}
	50	43.00^{ab}	56.67^{d}	70.67^{hij}	96.27^{n}
	100	43.67^{b}	58.67^{e}	72.00^{k}	117.32^{r}

Mean values with different lowercase superscripts are significantly ($p < 0.05$) different within each spraying altitude.

For the local drone with the sprayer arm, the results from the three-way analysis of variance revealed that main effects, the interaction between each two factor, as well as the interactions of all three factors had significant impacts on the spraying footprint. Fig. 4A shows that there was no interaction between the factors of the altitude of spraying (5 m, 7 m or 9 m) and the density of the yellow color (25%, 50% or 100%) at a nozzle altitude of 1 m. In contrast, interaction was clearly observed at the nozzle altitude levels of 2 m, 3 m and 4 m (Figs. 4B−4D). Notably, at a nozzle altitude level of 4 m, the effect of the density of the yellow color was apparent whereby only the density of 100% produced a high spray footprint (113.31−117.32 cm, Table 3). This was probably due to the low resolution of the camera used which resulted in reduced image segmentation efficiency at a low density of the yellow color. Consequently, the spraying footprint (Y) of the local drone with the sprayer arm was likely to decrease.

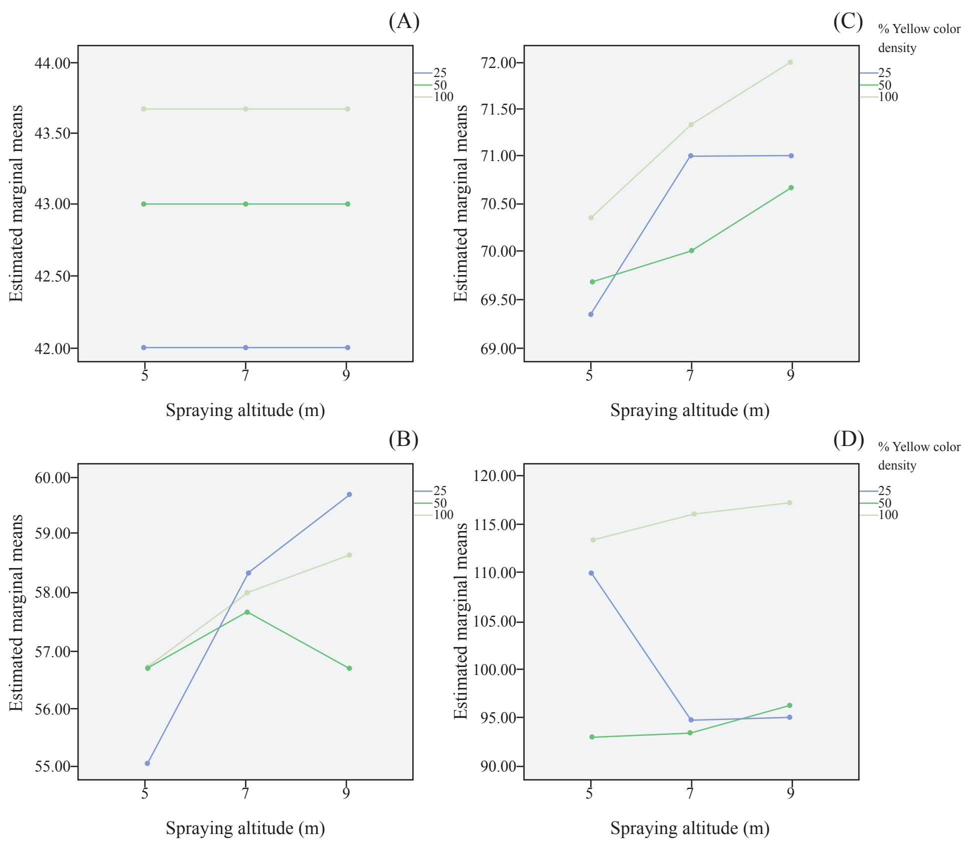

Fig. 4 Interaction between spraying altitude and density of yellow color sheet at different nozzle altitude levels: (A) 1 m; (B) 2 m; (C) 3 m; (D) 4 m

Overall, the highest spraying footprint was obtained using the three conditions of nozzle altitude of 4 m, with 100% yellow color density and spraying heights of 5 m, 7 m or 9 m. These conditions generated the highest spraying footprints (113.31 cm, 116.10 cm, and 117.32 cm, respectively), as shown in Table 3.

Variable rate sprayer

The spraying footprint was examined at nozzle altitudes of 0.5 m, 0.7 m, 1 m or 2 m and at a pressure of 0.15 MPa, with the resulting spraying flow rate being 162.72 L/hr. when the yellow color was applied with densities of 25% (13 pieces), 50% (26 pieces) or 100% (52 pieces), as shown in Table 4. The image data collecting and processing system using the wireless WebCAM was calibrated against the known values of color densities with yellow colors at various altitudes for the variable rate spraying system (5 m, 7 m and 9 m). The top canopy area of the palm at the spraying footprint was represented by these colored panels, which were utilized for calibration.

The three-way analysis of variance produced similar results with those for the local drone with the sprayer arm in that all factors (altitude of spraying, density of yellow color and nozzle altitude level) and their interactions significantly affected the spraying footprint (Y) of the a variable rate sprayer. With 100% yellow color density, spraying heights of 5 m, 7 m and 9 m had acceptable high accuracy in the image processing data and the spraying area, measuring 70.33 cm, 71.33 cm and 72.0 cm, respectively.

Fig. 5 shows the interactions of the spraying altitude and the density of yellow color at different nozzle altitudes. Different graph configurations among different nozzle altitudes (Fig. 5A−5D) clearly demonstrated the interaction among the three factors. Therefore, the results of each factor combination were considered separately. As such, the highest spraying footprints were obtained from the combination of 1 m nozzle altitude at either 5 m, 7 m or 9 m spraying altitude for all color densities but with one exception at the 25% yellow color sheet density (Table 4). However, the spraying footprints obtained were clearly less than those obtained from the local drone with the sprayer arm.

Drone machine performance with remote controlled sprayer arm and variable rate sprayer

Local drone with remote controlled sprayer arm

The results revealed a relationship between the amount of electricity consumed and the speed at which the sprayer moved. Spraying rates of 0.268 L/hr, 0.333 L/hr, 0.841 L/hr and 1.042 L/hr were required while moving at 1 km/hr, 1.25 km/hr, 2 km/hr and 2.5 km/hr, respectively. The sprayer's operating capacities at the four speeds assessed were 0.284 ha/hr, 0.352 ha/hr, 0.154 ha/hr and 0.162 ha/hr, respectively, while the quantity of electricity utilized was 0.598 kWhr, 0.741 kWhr, 0.324 kWhr and 0.341 kWhr, as shown in Fig. 6 (Jayasuriya and Sangpradit, 2014 and Soni et al., 2016).

A sign of stress or infection in coconut palms is less chlorophyll than in healthy plants because the infected palms have a low moisture content, resulting in less absorbance of reflectance energy in the infrared region of the electromagnetic spectrum, while also lowering their reflectivity, with dead coconut trees having the lowest spectral reflectance (Jusoff et al., 2009). Cross comparison was carried out for data from the SPAD 502 chlorophyll meter (Fig. 7). Coconut trees that were mature and in good condition showed a substantial association between their chlorophyll content measured using the chlorophyll meter and that measured by $NDVI_{Drone}$ (r = 0.7885). A similar result was revealed for the infected mature coconut trees (r = 0.7971). Additionally, the correlation between the $NDVI_{Drone}$ and the $GNDVI_{Drone}$ was only slightly higher (r = 0.8126), perhaps because there was a strong correlation between the value of the "G" spectral band and the color of the mature coconut leaves that were healthy or infected (Fig. 8).

Table 4 Spraying footprint diameter (in centimeters) of variable rate sprayer at different spraying and nozzle altitudes and yellow color sheet density percentages

Spraying altitude (m)	Density of yellow color (%)	Nozzle altitude (m)			
		0.5	0.7	1	2
5	25	32.00^{a}	41.00^{g}	42.55^{hij}	56.10^{n}
	50	33.00^{b}	43.67^{klm}	43.22^{ijklm}	58.10^{o}
	100	37.67^{e}	42.67^{ijk}	44.12^{m}	56.55^{n}
7	25	35.00^{c}	42.33^{hi}	43.11^{ijkl}	59.00^{op}
	50	32.00^{a}	41.67^{gh}	43.54^{jklm}	58.42^{op}
	100	34.67^{c}	43.11^{ijkl}	42.86^{ijk}	59.11^{p}
9	25	36.12^{d}	41.07^{g}	42.44^{hi}	60.00^{q}
	50	39.20^{f}	42.27^{hi}	43.24^{ijklm}	57.00^{n}
	100	39.87^{f}	43.17^{ijklm}	44.00^{lm}	61.00^{r}

Mean values with different lowercase superscripts are significantly ($p < 0.05$) different within each spraying altitude.

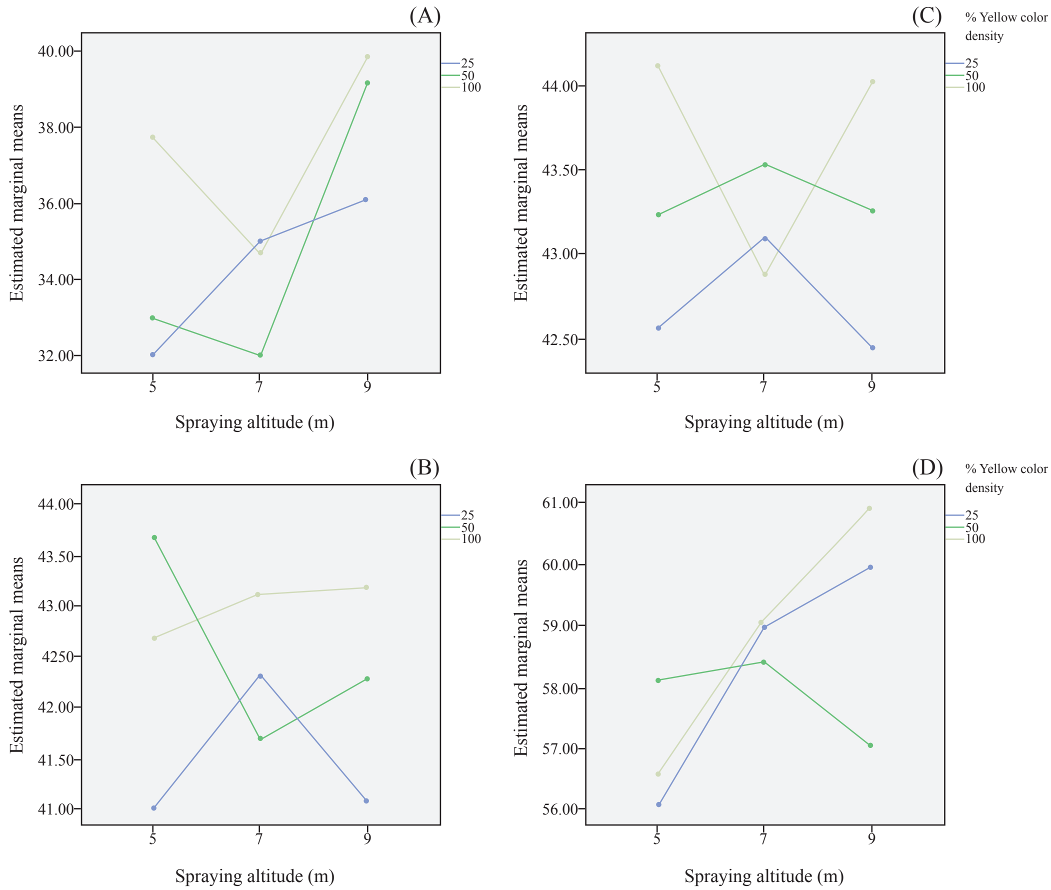

Fig. 5 Interaction between the altitude of spraying and density of yellow color sheets at different nozzle altitude levels: (A) 0.5 m; (B) 0.7 m; (C) 1.0 m; (D) 2.0 m

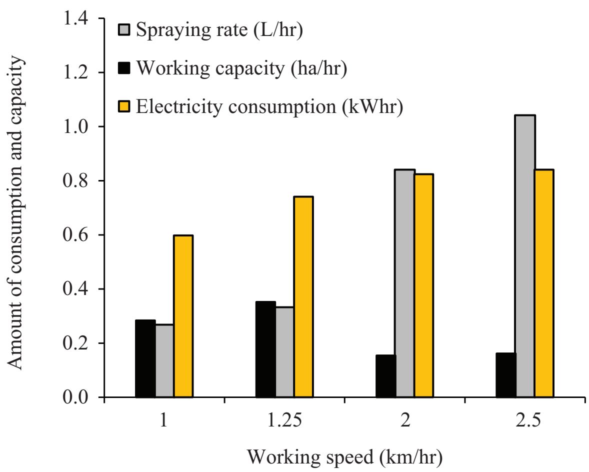

Fig. 6 Field performance of local drone with remote controlled sprayer arm

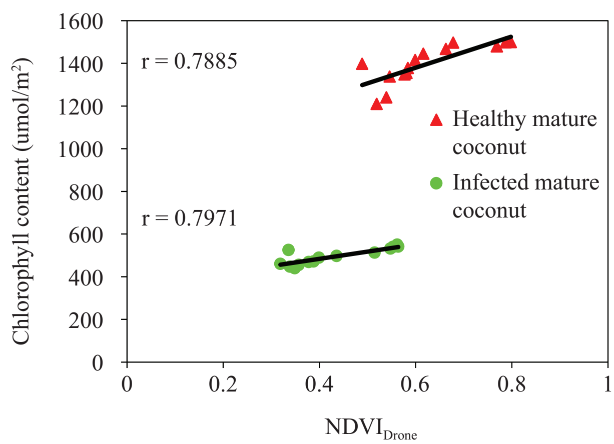

Fig. 7 Correlation between chlorophyll content measured using chlorophyll meter and normalized difference vegetation index measured using drone ($NDVI_{Drone}$) in healthy and infected coconut palms, where r = Pearson's correlation coefficient

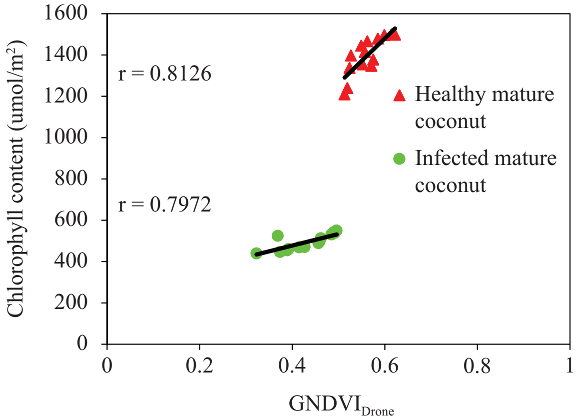

Fig. 8 Correlation between chlorophyll content measured using chlorophyll meter and green normalized difference vegetation index measured using drone ($GNDVI_{Drone}$) in healthy and infected coconut trees, where r = Pearson's correlation coefficient

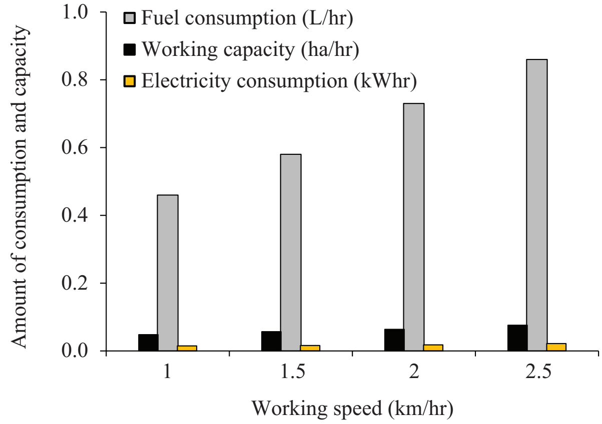

Fig. 9 Field performance of variable rate sprayer

Variable rate sprayer

The results demonstrated a direct correlation between fuel use and the speed at which the sprayer moved. While traveling at 1 km/hr, 1.5 km/hr, 2 km/hr and 2.5 km/hr fuel was used at rates of 0.46 L/hr, 0.58 L/hr, 0.73 L/hr and 0.86 L/hr, respectively. At these four speeds tested, the sprayer's working capacity was 0.048 ha/hr, 0.057 ha/hr, 0.064 ha/hr and 0.076 ha/hr, respectively, and the amount of power used was 0.015 kWhr, 0.016 kWhr, 0.018 kWhr and 0.022 kWhr, respectively (Fig. 9).

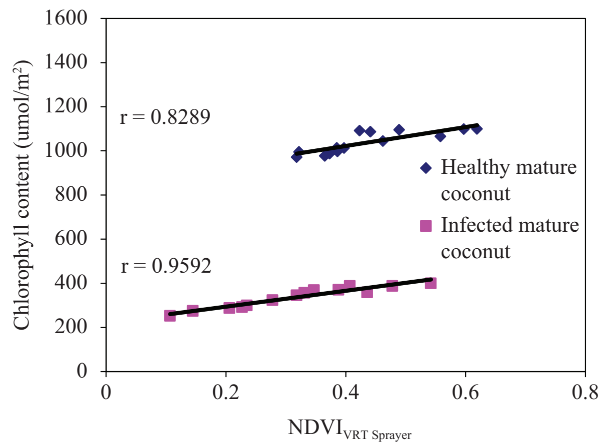

Fig. 10 Correlation between chlorophyll content measured using chlorophyll meter and normalized difference vegetation index measured using variable rate sprayer ($NDVI_{VRT\ Sprayer}$) in healthy and infected coconut trees, where r = Pearson's correlation coefficient

Correlation between plant canopy reflectivity (healthy or infected) and chlorophyll content

Variable rate sprayer

For healthy mature coconut trees, the correlation was reasonable (r = 0.8289) between the chlorophyll content measured using the chlorophyll meter and using the $NDVI_{VRT\ Sprayer}$ measured using the radiance at the leaf surface. Furthermore, for the infected mature coconut palms, the chlorophyll content measured using the $NDVI_{VRT\ Sprayer}$ was highly correlated (r = 0.9592) with the value recorded using the chlorophyll meter (Fig. 10). In addition, the $GNDVI_{VRT\ Sprayer}$ had a somewhat higher correlation (r = 0.8288 and r = 0.9595) than the $NDVI_{VRT\ Sprayer}$ (r = 0.8289 and r = 0.9592). This may have been related to the close relationship between the value of the "G" spectral band and the greenness of the healthy and infected mature coconut leaves, as shown in Fig. 11 (Jayasuriya et al., 2014 and Soni et al., 2016).

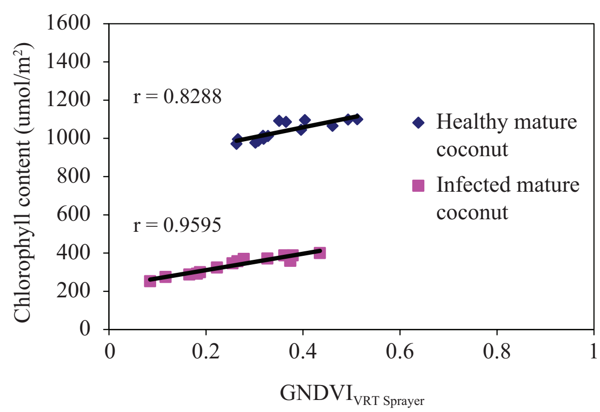

Fig. 11 Correlation between chlorophyll content measured using chlorophyll meter and green normalized difference vegetation index measured using variable rate sprayer ($GNDVI_{VRT\ Sprayer}$) in healthy and infected coconut trees, where r = Pearson's correlation coefficient

Coconut infected mapping

The results showed that test plots measuring 40 m × 40 m should be divided into smaller sub-plots measuring 7.8 m × 7.8 m to collect data and GPS coordinates using the handheld Garmin unit for latitude and longitude while monitoring the SPAD 502 chlorophyll meter readings. Later, using the ArcGIS® software, GIS application mapping of the chlorophyll content (at 3 mth and 6 mth) that comprised geographic data about the test area was produced (Astanakulov et al., 2021). Fig. 12 demonstrates the high apparent infection level, as well as the uniform distribution of the displayed chlorophyll content values.

The advantage of using the local drone with the remote-controlled sprayer arm was that spraying could be done swiftly while covering a larger number of coconut trees for each run, especially when the coconut plantation was located in an area with plenty of water, where the setup worked extremely well. However, the downsides were that the setup could only carry a modest quantity of chemical reagents and could only work for up to 15 min per battery at a time. On the other hand, the spraying rate was very low for the VRT sprayer, so the operation covered fewer coconut palms each injection time. Spraying is challenging in areas where the coconuts are is located in a garden with a lot of water; however, spraying can be conducted all day and the unit was strong and could easily transported a lot of chemical.

Conclusions

A drone with remote controlled sprayer arm was successfully developed and was shown to have improved efficiency over the VTR sprayer. The spraying rate of 0.333 L/hr for the local drone with a working speed of 1.25 km/hr resulted in 0.741 kWhr electricity consumption and a working capacity of 0.352 ha/hr.

Spraying footprints from drone were highest when operated at altitudes of either 5 m, 7 m or 9 m with 100% density of yellow color and a nozzle altitude of 4 m (spraying footprint diameter range = 113.31−117.32 cm). The footprints obtained using the VTR sprayer were much smaller than those of drones with highest VTR spraying footprint diameters in the range 69.67−72.00 cm.

There was a strong correlation between the amount of chlorophyll measured using the SPAD 502 chlorophyll meter and the normalized difference vegetation index captured by the drone ($NDVI_{Drone}$) of healthy (r = 0.7885) and infected (r = 0.7971) coconuts. Additionally, when using the $GNDVI_{Drone}$ instead of the $NDVI_{Drone}$, comparable correlation coefficients were obtained in both healthy and infected trees (r = 0.8126 and 0.7972, respectively).

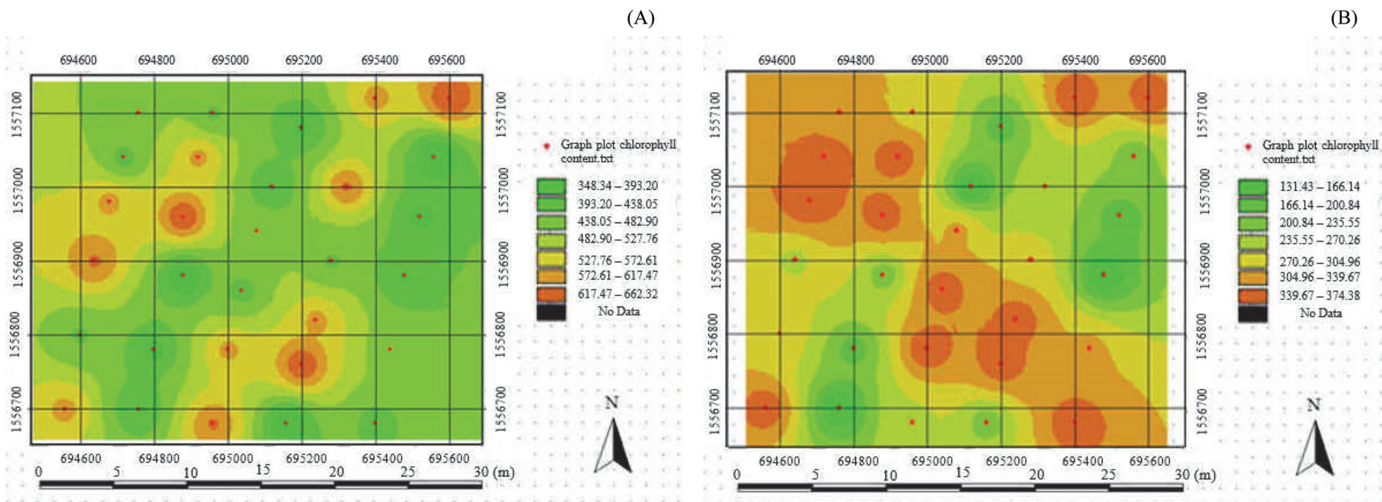

Fig. 12 Infected coconut mapping based on coconut palm chlorophyll content at: (A) 3 mth; (B) 6 mth

The VRT sprayer was constructed and operated with a working capacity of 0.056 ha/hr and a spraying rate of 162.72 L/hr at a forward speed of 1.5 km/hr and fuel consumption of 0.58 L/hr. The chlorophyll content measured using the chlorophyll meter was well correlated with $NDVI_{VRT\ Sprayer}$ (r = 0.8289 and r = 0.9592 for healthy and infected trees, respectively). The level of correlation was unchanged when $GNDVI_{VTR\ Sprayer}$ was used (r = 0.8288 and 0.9595 for healthy and infected trees, respectively).

Conflict of Interest

The authors declare that there are no conflicts of interest.

Acknowledgments

The authors thank the local farmer in Pathum Thani, Bueng Bon, Nong Suea district who donated the experimental infrastructure. Financial support for this work was provided by Rajamangala University of Technology Thanyaburi (RMUTT), Faculty of Engineering, Agricultural Engineering, Klong 6, Thanyaburi, Pathumthani, Thailand.

References

Astanakulov, K., Shovazov, K., Borotov, A., Turdibekov, A., Ibrokhimov, S. 2021. Wheat harvesting by combine with GPS receiver and grain sensor. E3S Web of Conferences 227: 07001. doi.org/10.1051/e3sconf/202122707001

Gitelson, A.A., Kaufman, Y.J., Merzlyak, M.N. 1996. Use of a green channel in remote sensing of global vegetation from EOS-MODIS. Remote Sens. Environ. 58: 289–298. doi.org/10.1016/S0034-4257(96)00072-7

Indarto, I., Rahayu, C.U., Soekarno, S. 2022. Land cover mapping using Sentinel-2 images in area dominated by small-scale, heterogeneous agricultural parcels. Agr. Nat. Resour. 56: 233–242. doi.org/10.34044/j.anres.2022.56.2.02

Jarimopas, B., Jaisin, N. 2008. An experimental machine vision system for sorting sweet tamarind. J. Food Eng. 89: 291–297. doi.org/10.1016/j.jfoodeng.2008.05.007

Jusoff, K., 2009. Mapping of Sabah Islands using airborne hyperspectrometer. Journal of Geography and Geology 1: 2. doi: 10.5539/jgg.v1n1p2

Jayasuriya, H.P., Sangpradit, K. 2014. Dynamic performance and ride comfort evaluation of the seat suspension system in a small agricultural tractor to attenuate low-frequency vibration transmission. Agric. Eng. Int. CIGR Journal 16: 207–216. https://cigrjournal.org/index.php/Ejounral/article/view/2238/1855

Markwell, J., Osterman, J.C., Mitchell, J.L. 1995. Calibration of the Minolta SPAD-502 leaf chlorophyll meter. Photosynth. Res. 46: 467–472. doi.org/10.1007/BF00032301

Office of Agricultural Economics. 2020. Ministry of Agriculture and Cooperatives. Agricultural Economic Basic Information. 2020. http://www.oae.go.th, 9 November 2020.

Sirisomboon, P., Hashimoto, Y., Tanaka, M. 2009. Study on non-destructive evaluation methods for defect pods for green soybean processing by near-infrared spectroscopy. J. Food Eng. 93: 502–512. doi.org/10.1016/j.jfoodeng.2009.02.019

Samseemoung, G., Jayasuriya, H.P., Soni, P. 2011. Oil palm pest infestation monitoring and evaluation by helicopter-mounted, low altitude remote sensing platform. J. Appl. Remote Sens. 5: 053540. doi.org/10.1117/1.3609843

Samseemoung, G., Sangpradit. K., Pinthong, A. 2016. Development of a remote control system for orchid diseases monitoring using image processing technique for precision application of chemicals in standard greenhouses. Thai Society of Agricultural Engineering Journal 22: 7–20. https://li01.tci-thaijo.org/index.php/TSAEJ/article/view/68886

Samseemoung, G., Soni, P., Jayasuriya, H.P., Salokhe, V.M. 2012. Application of low altitude remote sensing (LARS) platform for monitoring crop growth and weed infestation in a soybean plantation. Precision Agric. 13: 611–627. doi.org/10.1007/s11119-012-9271-8

Samseemoung, G., Soni, P., Suwan, P. 2017a. Development of a variable rate chemical sprayer for monitoring diseases and pests infestation in coconut plantations. Agriculture 7: 89. doi.org/10.3390/agriculture7100089

Samseemoung, G., Soni, P., Sirikul, C. 2017b. Monitoring and precision spraying for orchid plantation with wireless WebCAMs. Agriculture 7: 87. doi.org/10.3390/agriculture7100087

Samseemoung, G., Thongindam, P., Soni, P., 2023. Drone application with low-cost remote-controlled earth-drilling machine for modern agriculture. Agr. Nat. Resour. 57: 173–180. doi.org/10.34044/j.anres.2023.57.1.18

Sirikun, C., Samseemoung, G., Soni, P., Langkapin, J., Srinonchat, J. 2021. A grain yield sensor for yield mapping with local rice combine harvester. Agriculture 11: 897. doi.org/10.3390/agriculture11090897

Soni, P., Salokhe, V.M. 2016. Bio-inspired macro-morphologic surface modifications to reduce soil–tool adhesion. In: Ng, E.Y.K., Luo, Y. Bio-Inspired Surfaces and Applications. World Scientific. 5 Toh Tuck Link, Singapore, pp. 421–484. doi.org/10.1142/9789814704496_0012